

High-Resolution Study of Isomer Shifts of the 6.2-keV γ Rays of Tantalum-181*

G. Kaindl† and D. Salomon

Lawrence Berkeley Laboratory, University of California, Berkeley, California 94720

G. Wortmann

Physik-Department E15, Technische Universität München, D-8046 Garching, Germany.

(Received 2 April 1973)

Isomer shifts of the 6.2-keV γ rays of ^{181}Ta are reported for dilute impurities of tantalum in transition-metal hosts and for several tantalum compounds. The experimental line-shift-to-linewidth ratios represent an improvement of the resolution by more than an order of magnitude relative to other Mössbauer resonances. For ^{181}Ta impurities in transition-metal hosts a systematic variation of the electron density at the nucleus is found. From a comparison of the isomer shifts of ^{181}Ta impurities in transition-metal host with those observed for impurities of ^{57}Fe , ^{99}Ru , ^{193}Ir , and ^{197}Au , a value of $\Delta\langle r^2 \rangle = -5 \times 10^{-2} \text{ fm}^2$ can be derived for the change of the mean-squared nuclear-charge radius. The negative sign of $\Delta\langle r^2 \rangle$ is in agreement with the observed variation of the isomer shifts of LiTaO_3 , NaTaO_3 , and KTaO_3 , as well as with the isomer shift found for TaC.

I. INTRODUCTION

Relatively low resolution is usually considered as one of the drawbacks of Mössbauer investigations of hyperfine interactions. In efforts to improve this, considerable interest has therefore been drawn to the few Mössbauer resonances with lifetimes in the μsec region, as those of ^{67}Zn ¹ and ^{181}Ta .²⁻⁴ While the 90-keV γ resonance of ^{67}Zn ($T_{1/2} = 9.3 \mu\text{sec}$) should ultimately provide superior opportunities for studying relativistic effects, the 6.2-keV γ resonance of ^{181}Ta ($T_{1/2} = 6.8 \mu\text{sec}$) may be considered as the top candidate for high-resolution Mössbauer spectroscopy applied to the study of hyperfine interactions, owing to the large magnitudes of its pertinent nuclear parameters. It has been shown recently that this is both true for magnetic dipole^{3,5-7} and electric quadrupole^{5,8-10} hyperfine interactions.

The special features of the 6.2-keV γ resonance, however, are most clearly demonstrated in the field of isomer shifts, as will be shown in the present paper. Until very recently, the only lattice in which isomer shifts had been observed with this γ resonance, were tungsten and tantalum metal.²⁻⁴ We have now studied isomer shifts for ^{181}Ta impurities in several of the $5d$, $4d$, and $3d$ transition metals, and for a few tantalum compounds. The observed isomer shifts cover a total range of 110 mm/sec, which may be compared with twice the natural width of the 6.2-keV γ rays, $W_0 = 2\hbar/\tau = 0.0064 \text{ mm/sec}$, or at least with the best experimental linewidth observed up to now, $W_{\text{expt}} = 0.069 \text{ mm/sec}$.¹¹ The present results represent an improvement of the resolution obtained with the Mössbauer method by more than an order of magnitude.

In part, this paper is a summary of data pre-

sented previously with an emphasis on different aspects in the form of letters, conference reports, and laboratory reports.⁵⁻¹⁵ It also contains, however, new data and a systematic evaluation of all the isomer-shift results obtained hitherto.

This paper will be presented in five sections. The experimental technique is discussed in Sec. II, while the experimental results are presented in Sec. III. Section IV contains the discussion and the derivation of a value for $\Delta\langle r^2 \rangle$ from isomer-shift systematics in transition-metal hosts. Finally, Sec. V presents the summary and conclusion.

II. EXPERIMENTAL TECHNIQUE

High-resolution Mössbauer spectroscopy requires refined experimental techniques. The Mössbauer resonance line can be "hyperfine broadened" by inhomogeneities of magnetic dipole and electric quadrupole interactions, as well as by local variations of the total electron density at the nucleus. The 6.2-keV γ resonance is particularly sensitive to impurities and lattice imperfections, requiring special care in the preparation of sources and absorbers.

A. Preparation of Sources

The 6.2-keV level of ^{181}Ta is populated by electron-capture decay of ^{181}W ($T_{1/2} = 140 \text{ days}$). For the present work samples of 93%-enriched ^{180}W metal were irradiated for periods up to 8 weeks in integrated thermal neutron fluxes ranging from 10^{21} n/cm^2 to as much as 10^{22} n/cm^2 , resulting in ^{181}W of high specific activity. The source preparation process can be divided into several steps, namely, preparation of the host-metal disks, deposition of the ^{181}W activity, reduction of the W deposit in hy-

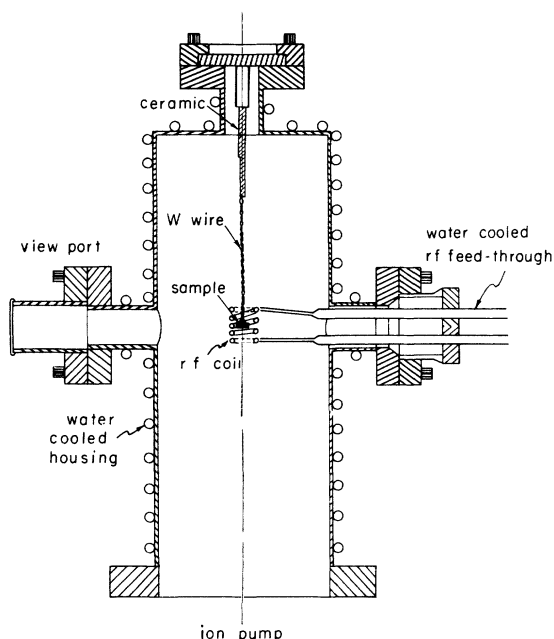


FIG. 1. Schematic drawing of the high-vacuum source preparation chamber.

drogen atmosphere, and diffusion in high vacuum at elevated temperatures.

The metal samples were prepared from high-purity and, if available, single-crystal materials. Single crystals were used to ensure high purity and to preclude preferential diffusion along grain boundaries. With a spark cutter, disks of about 1-mm thickness and typically 6 mm in diameter were cut from bulk samples. In case of the hexagonal metals Re, Ru, and Hf, oriented disks were cut from single crystals. The metal samples were mechanically polished, etched, and, if possible, finally electropolished.

After irradiation, the tungsten activity was dissolved in a few drops of 1:1 mixture of concentrated HF : HNO₃. The solution was then diluted with water, evaporated to dryness, and the residue again dissolved in water. Since tungsten does not easily electroplate, the activity was dropped onto the metal disks and dried.

The consecutive reduction and diffusion process was carried out in a high-vacuum source-preparation chamber, shown schematically in Fig. 1. The sample was hung horizontally into the center of a water-cooled rf coil. Through a view port the temperature of the sample could be measured with a pyrometer. In all cases but palladium, the tungsten activity was first reduced in hydrogen atmosphere at 950 °C for about ½ h. Diffusion was then performed in high vacuum of 10⁻⁸–10⁻⁹ Torr at various temperatures and for various periods. Specific information on the preparation of the sources is

presented in Table I.

Several sources (W, Ta, Mo, Nb, Pt, and V) were also prepared by resistance heating of foils or single-crystal disks in a similar way to that described by Sauer.⁴ The rf-heating method, however, was found to be more appropriate for single-crystal samples. The use of foils leads to the problem that they may become brittle or may break at relatively low temperatures compared to the melting point.

B. Preparation of Absorbers

Absorbers for experiments with the 6.2-keV γ resonance ought to be prepared from high-purity materials, and should have a small thickness and a high homogeneity because of the large photoelectric cross section of tantalum for the 6.2-keV γ rays. In the present work absorbers were prepared from tantalum metal and from several tantalum compounds.

The high-vacuum annealing and degassing procedure, employed for preparing the tantalum-metal absorber, was very similar to the one described previously by Sauer.⁴ The Ta foil was heated resistively in an arrangement similar to the source preparation chamber (Fig. 1). As a starting material a foil of 99.996% purity and 13- μ thickness was used. It was initially outgassed in a vacuum of about 10⁻⁹ Torr and temperatures up to 2300 °C for 20 h. The foil was then alternately rolled between a sandwich of similarly prepared Ta foils,

TABLE I. Summary of source preparation data, including information on the nominal purity of the host metals, their crystalline state (sc: single crystal; pc: polycrystalline), and the methods used for cleaning the surfaces.

Host metal	Nominal purity (%)	Surface cleaning	Diffusion temperature (°C)	Diffusion time (h)
Hf, sc	99.9	a	1600	8
Ta, sc	99.999	a	2500	1
W, sc	99.999	b	2500	0.5
Re, sc	99.996	a	2400	1
Os, pc	99.9	a	2350	1
Ir, pc	99.99	c	1850	20
Pt, pc	99.99	c	1750	1
Nb, sc	99.99	a	2200	1
Mo, sc	99.99	a	2300	1
Ru, sc	99.99	d	2050	1
Rh, sc	99.99	a	1950	1
Pd, sc	99.98	a	1300	10
V, pc	99.9	a	1750	1
Ni, sc	99.995	a	1350	20

^aElectropolishing in 5% perchloric acid at dry-ice temperature (Ref. 16).

^bElectropolishing in 10% NaOH at about 40 °C.

^cSample was heated in air to about 1200 °C.

^dSample was treated in fused NaOH at about 350 °C.

and annealed again in vacuum at temperatures as high as possible. This procedure was repeated until a thickness of 4 mg/cm^2 was reached.

Absorbers of TaC , KTaO_3 , NaTaO_3 , and LiTaO_3 were prepared by a sedimentation method. At first the finer fraction of a ground powder was separated by sedimentation in alcohol. This material was then sedimented in a polystyrene-benzene solution on a $6\text{-}\mu$ -thick Mylar foil. During drying, a thin polystyrene film, containing the Ta compound in a relatively homogeneous layer, formed on the Mylar.

The alkali tantalates were of nominal 99.9% purity and were obtained from Research Organic/Inorganic Chemical Corp., Sun Valley, Calif. Two different samples of almost stoichiometric TaC were investigated,¹⁷ resulting in very similar resonance spectra.

C. Mössbauer Apparatus

All of the Mössbauer experiments reported here were performed in standard transmission geometry with fixed absorbers and sinusoidally moved sources. Both sources and absorbers were kept at room temperature, with the exception of the

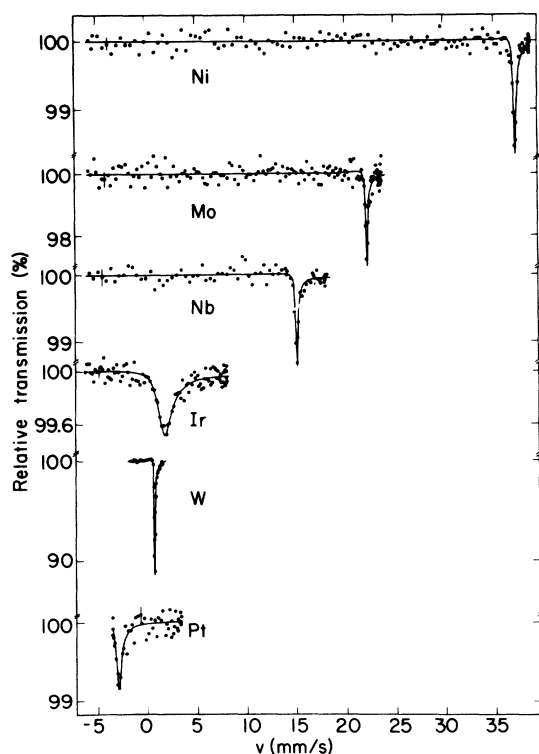


FIG. 2. Single-line absorption spectra of the 6.2-keV γ rays, obtained with a tantalum-metal absorber and sources of ^{181}W diffused into various cubic transition-metal hosts. The solid lines represent the results of least-squares fits of dispersion-modified Lorentzians to the data.

$\text{Ni}(^{181}\text{W})$ source.^{7,21}

The 6.2-keV γ rays were detected with an argon-filled proportional counter. Despite a much better energy resolution, a lithium-drifted Si detector was found inferior to the proportional counter for the present purpose because of high counting rates. A slight improvement in the background and consequently in the observed resonance effect could be obtained with an argon-10%-krypton proportional counter.

In cases with a large line-shift-to-linewidth ratio, as with Mo, Nb, Ni, and Re hosts, small solid angles were employed for the experiments in order to prevent excessive geometrical linebroadening.¹⁴ Then, the data were recorded with as many as 2048 channels, using a conventional sinusoidal velocity drive¹⁸ of high stability.

III. EXPERIMENTAL RESULTS AND DATA ANALYSIS

The present experiments may be divided into source and absorber experiments. In the former, the hyperfine splitting of the 6.2-keV γ rays emitted from dilute impurities of ^{181}Ta in transition-metal hosts was investigated using a single-line tantalum-metal absorber. In the latter cases, Mössbauer spectra were measured for absorbers of tantalum compounds with the help of a $\text{W}(^{181}\text{W})$ source.

A. Isomer Shifts for Dilute Impurities of ^{181}Ta in Transition Metals

The isomer shifts reported here were derived from single-line and split spectra. Some representative single-line spectra for metallic sources are shown in Fig. 2. The large range of observed isomer shifts is clearly demonstrated.

The pronounced asymmetry of the line shape results from an interference between photoelectric absorption and Mössbauer absorption followed by internal conversion.^{19,20} This effect was first experimentally observed by Sauer *et al.*,³ and has been found to be particularly large for the 6.2-keV γ rays of ^{181}Ta due to their E1 multipolarity, their low transition energy, and their large internal-conversion coefficient.

Following the theory of Trammel and Hannon¹⁹ the absorption spectra were fitted with dispersion-modified Lorentzian lines of the form

$$N(v) = N(\infty) \left[1 - \epsilon(1 - 2\xi X) / (1 + X^2) \right], \quad (1)$$

with $X = 2(v - S)/W$. Here $N(v)$ is the intensity transmitted at relative velocity v , S is the position of the line, W is the full linewidth at half-maximum, and ϵ is the magnitude of the resonance effect. The parameter ξ determines the relative magnitude of the dispersion term.

As has been shown previously,^{5,15} the experimental result $2\xi = -0.31 \pm 0.01$, derived both from

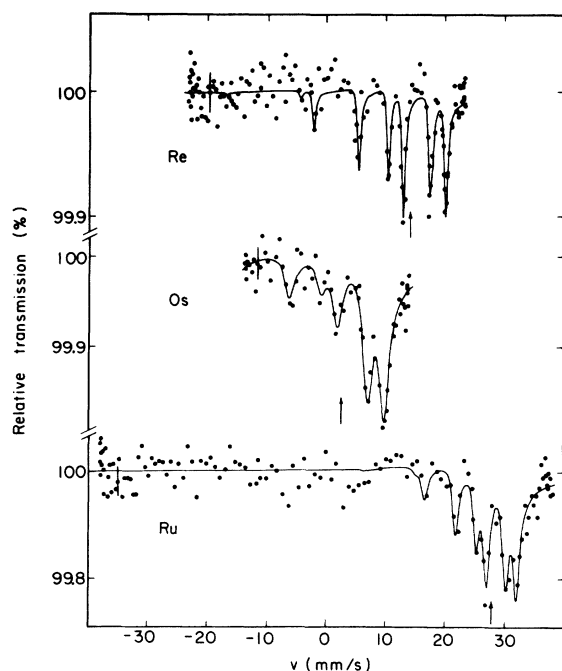


FIG. 3. Electric quadrupole split-absorption spectra of the 6.2-keV γ rays for sources of ^{181}W diffused into hexagonal transition metals. The isomer shifts relative to a tantalum-metal absorber are indicated by arrows.

single-line and magnetically split spectra, agrees very well with the theoretical value predicted in Ref. 19. Consequently, all the spectra of the present work were fitted with a constant amplitude of the dispersion term $2\xi = -0.31$.

In the case of sources diffused into the hexagonal transition metals Re, Os, Hf, and Ru, the emission spectra are split by electric quadrupole interaction as reported earlier.^{8,9} In an axially symmetric electric field gradient the $\frac{3}{2}^- \rightarrow \frac{1}{2}^+$ E1 transition splits into 11 hyperfine components. Some representative spectra are shown in Fig. 3. While the spectrum for osmium was obtained with a polycrystalline source, both the rhenium and ruthenium spectra were measured with single-crystal sources of $\text{Re}(^{181}\text{W})$ and $\text{Ru}(^{181}\text{W})$, respectively, with direction of observation perpendicular to the hexagonal c axis. The solid lines in Fig. 3 are the results of least-squares fits of superpositions of dispersion-modified Lorentzians to the data. In addition to $2\xi = -0.31$, the ratio of quadrupole moments was also kept constant and set equal to the result of Ref. 8, $Q(\frac{3}{2})/Q(\frac{1}{2}) = 1.133 \pm 0.010$.

The isomer-shift results (S) for dilute impurities of ^{181}Ta in transition-metal hosts, with both sources and absorbers at room temperature, are summarized in Table II. The value quoted for the nickel host was extrapolated from the temperature dependence of the line position, as measured above

the Curie point of nickel.²¹ The isomer shifts are defined in a way that a more positive value corresponds always to a larger transition energy.

The observed experimental linewidths W range from about 11 times twice the natural width in the case of the tungsten source up to about 800 times in the case of the vanadium source. The narrowest linewidths have been observed for those host metals which are continuously miscible with tantalum metal (with the exception of V). The best line-shift-to-linewidth ratios were found for the Mo, Nb, and Ni hosts, even though the experimental linewidths for these sources are from 20 to 77 times the theoretical minimum.

Results similar to ours were obtained by other groups only for the tungsten and tantalum hosts,^{2-4,22} and their data agree well with the present results.

B. Isomer Shifts for Tantalum Compounds

Tantalum occurs in the pentavalent, tetravalent, and trivalent state.²³ However, only the pentavalent compounds and a few hard refractory metals^{23,24} are stable enough to allow an investigation with the present experimental technique. In this study, Mössbauer absorption spectra have been measured at room temperature for the alkali tantalates LiTaO_3 , NaTaO_3 , and KTaO_3 , and for TaC.

The results for the tantalates are presented in Fig. 4. For KTaO_3 , which has the cubic NaCl structure, a broadened single line is observed, while electric quadrupole split spectra are found

TABLE II. Summary of results for sources of ^{181}W diffused into various transition-metal hosts, with both sources and absorbers at room temperature. S is the isomer shift relative to tantalum metal, W is the experimental linewidth (FWHM), and ϵ is the magnitude of resonance effect, summed over all hyperfine components.

Source lattice	S (mm/sec)	W (mm/sec)	ϵ (%)
V	-33.2 ± 0.5	5.0 ± 1.0	0.1
Ni	-39.5 ± 0.2^a	0.50 ± 0.08	1.6
Nb	-15.26 ± 0.10	0.19 ± 0.06	1.5
Mo	-22.60 ± 0.10	0.13 ± 0.04	3.0
Ru	-27.50 ± 0.30	1.3 ± 0.2	0.7
Rh	-28.80 ± 0.25	3.4 ± 0.5	0.3
Pd	-27.80 ± 0.25	1.3 ± 0.3	0.3
Hf	-0.60 ± 0.30	1.6 ± 0.4	0.2
Ta	-0.075 ± 0.004	0.184 ± 0.006	2.4
W	-0.860 ± 0.008	0.069 ± 0.001	20
Re	-14.00 ± 0.10	0.60 ± 0.04	1.3
Os	-2.35 ± 0.04	1.8 ± 0.2	0.8
Ir	-1.84 ± 0.04	1.60 ± 0.14	0.5
Pt	$+2.66 \pm 0.04$	0.30 ± 0.08	1.5

^aExtrapolated to room temperature from the temperature dependence of the line position, measured for the $\text{Ni}(^{181}\text{W})$ source in the temperature range 685–1003 K (Ref. 21).

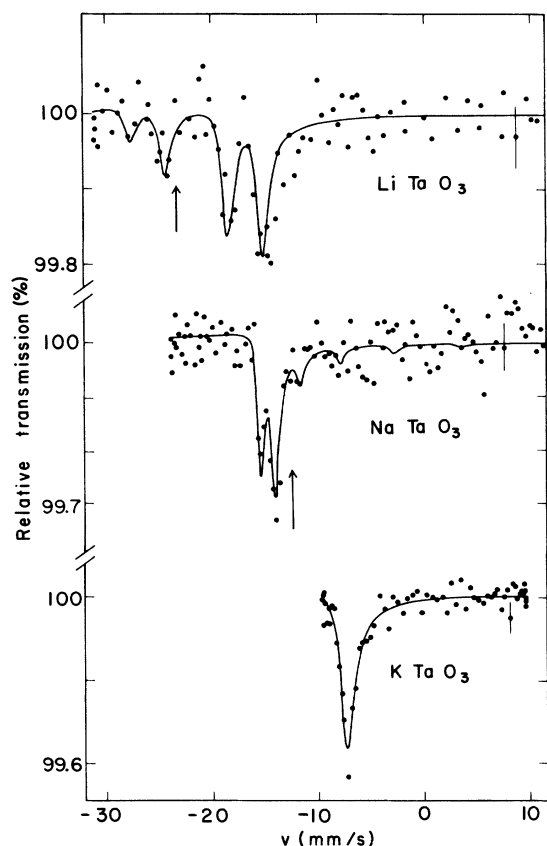


FIG. 4. Mössbauer absorption spectra for various alkali tantalates recorded with a source of $W^{181}W$. The centers of the electric quadrupole split spectra are indicated by arrows.

for hexagonal $LiTaO_3$ and orthorhombic $NaTaO_3$. The spectra for $LiTaO_3$ and $NaTaO_3$ were least-squares fitted with the assumption of an axially symmetric electric field gradient, and constant $Q(\frac{3}{2})/Q(\frac{1}{2}) = 1.133^8$; in this way, values for the isomer shifts as well as for the signs and magnitudes

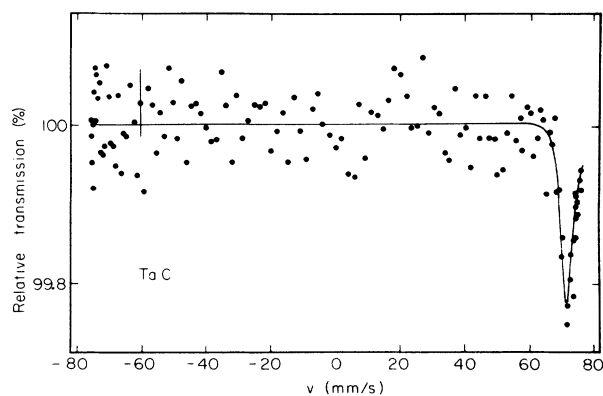


FIG. 5. Nuclear-resonance absorption of the 6.2-keV γ rays in TaC, measured with a $W^{181}W$ source.

TABLE III. Compilation of results for several tantalum compounds, with both sources and absorbers at room temperature. S is the isomer shift relative to tantalum metal, W is the experimental linewidth (FWHM), and ϵ is the magnitude of resonance effect, summed over all hyperfine components.

Compound	S (mm/sec)	W (mm/sec)	ϵ (%)
$LiTaO_3$	-24.04 ± 0.30	1.6 ± 0.2	0.9
$NaTaO_3$	-13.36 ± 0.30	1.0 ± 0.2	0.9
$KTaO_3$	-8.11 ± 0.15	1.5 ± 0.2	0.3
TaC	$+70.8 \pm 0.5$	2.4 ± 0.4	0.2

of the electric field gradients at the tantalum sites were obtained.¹⁰

Figure 5 shows the absorption spectrum of TaC measured with a $W^{181}W$ source. As expected from the cubic crystal structure of TaC, a single,

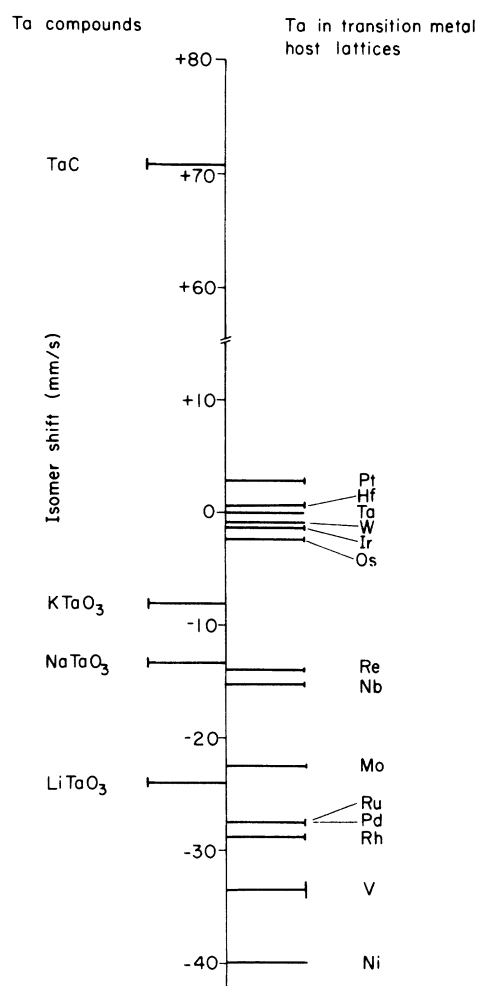


FIG. 6. Graphical representation of isomer shifts of the 6.2-keV γ rays for tantalum compounds and for dilute impurities of ^{181}Ta in transition-metal hosts.

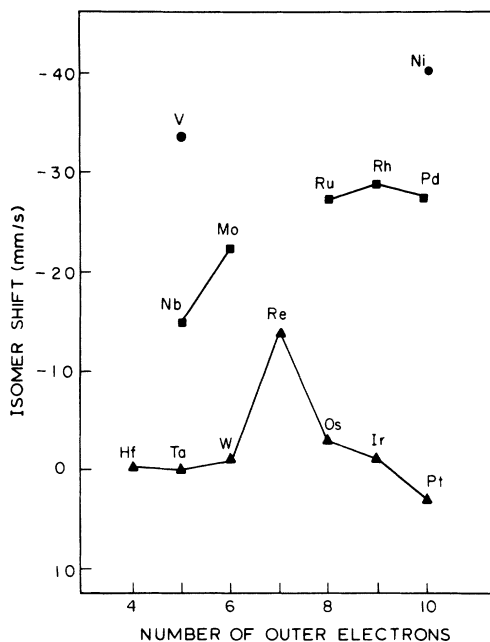


FIG. 7. Systematics of isomer shifts of the 6.2-keV γ rays for dilute impurities of ^{181}Ta in transition-metal hosts.

though broadened line is obtained. This spectrum exhibits the largest isomer shift observed so far.

Table III summarizes all of our isomer-shift results for compounds of tantalum. Two separate samples of KTaO_3 and of TaC^{17} were investigated with consistent results in both cases. The observed linewidths for all of the studied compounds are markedly wider than those of the best metallic systems. The present total range of isomer shifts of compounds of tantalum, however, is much larger than for metallic hosts, covering about 95 mm/sec.

C. Summary of Isomer-Shift Results

A graphical representation of the present isomer-shift results is shown in Fig. 6. The isomer shifts are plotted there separately for tantalum compounds and for dilute impurities of ^{181}Ta in transition-metal hosts. Recalling the used sign convention for isomer shifts, one realizes that the transition energy increases in this plot from bottom to top.

The total range of isomer shifts (110 mm/sec) corresponds to 17 000 times twice the natural width of the 6.2-keV γ rays or 1 600 times the best experimental linewidth obtained up to now. These numbers clearly demonstrate the high resolution with which solid-state effects on the electron density at the nucleus may be studied using this γ resonance.

IV. DISCUSSION

The present isomer-shift results for metallic hosts will be used in the following to derive in a comparative way a quantitative estimate for the change of the mean-squared nuclear-charge radius $\Delta\langle r^2 \rangle = \langle r^2 \rangle_e - \langle r^2 \rangle_g$ between the excited state and the ground state of ^{181}Ta . For this purpose, the systematic variation of electron densities (ρ) at the nuclei of ^{181}Ta , ^{57}Fe , ^{99}Ru , ^{193}Ir , and ^{197}Au impurity atoms in hosts of the 5d, 4d, and 3d transition metals is discussed in Sec. IV A. With certain assumptions these data are then used to derive ratios of $\Delta\langle r^2 \rangle$ of the ^{181}Ta γ resonance to those of the pertinent Mössbauer transitions of ^{57}Fe , ^{99}Ru , ^{193}Ir , and ^{197}Au . Using the known numbers for $\Delta\langle r^2 \rangle$ of these Mössbauer transitions a value for $\Delta\langle r^2 \rangle$ of the 6.2-keV γ transition is obtained. Finally, the isomer shifts found for tantalum compounds will be discussed qualitatively, and it can be shown that they strongly support a negative sign for $\Delta\langle r^2 \rangle$.

A. Systematics of Isomer Shifts in Transition Metal Hosts

The isomer shifts for dilute impurities of ^{181}Ta in transition-metal hosts exhibit systematic features when plotted, as in Fig. 7, versus the number of electrons in the valence shells of the various host elements. The data can be arranged in three groups corresponding to 3d, 4d, and 5d host metals. Without exception, the transition energy decreases when proceeding from a 5d to a 4d and further to a 3d host metal in the same column of the Periodic Table.

A similar systematic behavior has also been observed for isomer shifts of γ rays of ^{57}Fe (14.4 keV), $^{25}\text{ }^{99}\text{Ru}$ (90 keV), ^{197}Au (77 keV), and ^{193}Ir (73 keV).^{12,26-28} In all of these cases estimates for the changes of the mean-squared nuclear-charge radii $\Delta\langle r^2 \rangle$ are reasonably well established,²⁹ so that information on the systematic behavior of electronic densities at impurity nuclei may be derived from these data. This in turn can be used to estimate $\Delta\langle r^2 \rangle$ for the present ^{181}Ta γ resonance.

To allow such a comparison the data for impurities of ^{57}Fe , ^{99}Ru , and ^{197}Au are summarized in Fig. 8. The data for ^{99}Ru and ^{197}Au are taken from Refs. 12 and 26-28, while those for ^{57}Fe are taken from Refs. 25 and 30-32. The respective results of Ref. 28 for ^{193}Ir impurities have not been included in Fig. 8, but their systematic features closely resemble those for ^{99}Ru .

Taking the accepted signs of $\Delta\langle r^2 \rangle$ for the three γ resonances represented in Fig. 8,²⁹ it is clear that the electron densities at the nuclei of the various impurity atoms increase when going from a 5d

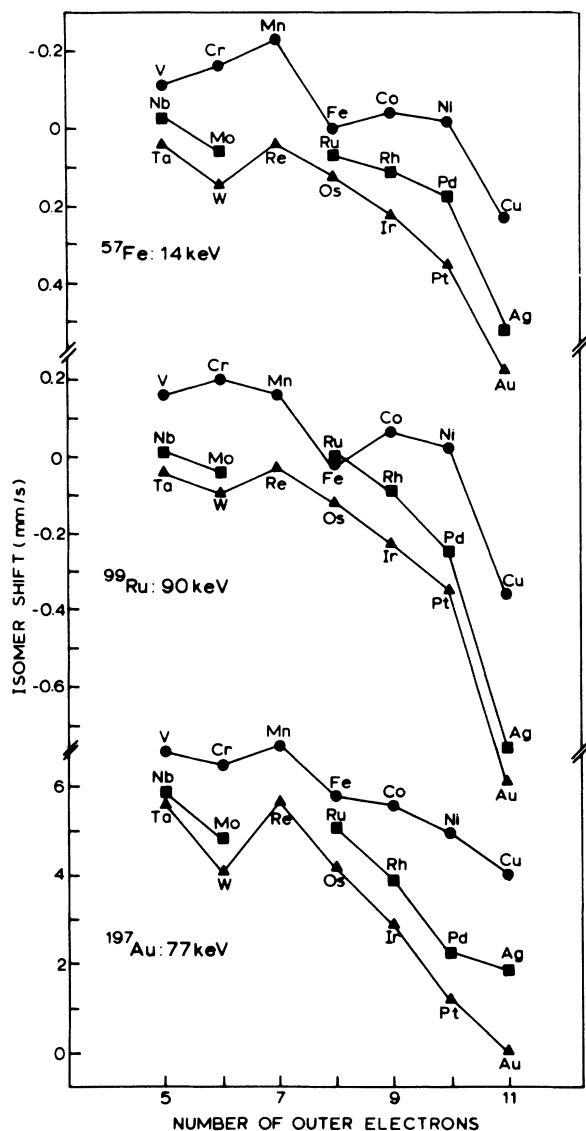


FIG. 8. Systematics of isomer shifts for dilute impurities of ^{57}Fe , ^{99}Ru , and ^{197}Au , measured with γ resonances of the impurity atoms at 14, 4, 90, and 77 keV, respectively.

via a $4d$ to a $3d$ host metal in a vertical column of the Periodic Table. The same conclusion has been drawn for impurities of ^{198}Ir .²⁸ The only exception to this rule is found for iron and its d -electron homologs, ruthenium and osmium, but in this column the lattice type changes from bcc to hcp. Such a systematic behavior of the electron density at the impurity atoms has been discussed theoretically by da Silva *et al.*³³ in connection with the ^{57}Fe data using a pseudopotential approach. They predicted a decrease in the d -electron density at the impurity atom from $5d$ to $4d$ to $3d$ host metals, which would cause an increase in ρ in agreement

with observation. A quantitative theoretical description of the charge transfer in Ag-Au alloys has recently been given by Gelatt and Ehrenreich.³⁴ The results presented in Figs. 7 and 8 and also those of Ref. 28 suggest that the electron density at the nucleus of transition-metal impurities in transition-metal hosts is generally increasing from a $5d$ to the homologous $4d$ and $3d$ host, respectively, with only very few exceptions. This finding leads to a negative value for $\Delta\langle r^2 \rangle$ of the 6.2-keV γ transition.

The dependence of ρ on the number of electrons N in the valence shell of the host elements of one transition series, however, is markedly different for impurity atoms of ^{181}Ta as compared to those of ^{57}Fe , ^{99}Ru , and ^{197}Au . While an over-all decrease of ρ with increasing N is observed for impurities of ^{57}Fe , ^{99}Ru , and ^{197}Au , ρ even increases slightly in the $4d$ series with increasing N in the case of ^{181}Ta . This dependence of ρ on N should reflect effects of the band structure, the atomic volume, and the lattice type of the host metals on the electronic structure of the impurity atoms. From band-structure effects a decrease in ρ with increasing N is expected, since the s character of the conduction bands of the hosts decreases in this direction.³⁵ On the other hand, the atomic volumes of the host metals, derived from lattice constants, exhibit a dependence on N which might contribute to the observed increase in ρ with N for ^{181}Ta impurities in $3d$ and $4d$ hosts, and in $5d$ hosts up to rhenium. The relative strengths of the various effects, however, seem to depend strongly on the nature of the impurity atoms.

B. Change of the Mean-Squared Nuclear-Charge Radius

In spite of these differences the observed systematic behavior of isomer shifts in transition-metal hosts may be employed to derive an estimate for the change of the mean-squared nuclear-charge radius $\Delta\langle r^2 \rangle$ of the 6.2-keV γ transition. As discussed above, changes of ρ within a column of homologous transition-metal hosts are much less affected by differences in the properties of impurity atoms than those within a transition series. In addition, the influence of the atomic volume of the host metal on ρ at the impurity atom is expected to be much less pronounced between homologous $4d$ and $5d$ hosts than between $3d$ hosts and any of the former ones. The reason for this is that the atomic volumes of homologous $4d$ and $5d$ metals are nearly the same, while those of homologous $3d$ metals are markedly different.³⁶ It seems appropriate therefore to compare only isomer-shift differences for homologous $5d$ and $4d$ host-metal pairs in order to derive ratios of $\Delta\langle r^2 \rangle$ of the ^{181}Ta γ resonance to those of the other γ resonances.

TABLE IV. (a) Isomer-shift differences between homologous $4d$ and $5d$ transition-metal hosts, measured with γ resonances of impurities of ^{181}Ta (6.2 keV), ^{197}Au (77 keV), ^{193}Ir (73 keV), ^{99}Ru (90 keV), and ^{57}Fe (14.4 keV). (b) Ratios of $\Delta S(^{181}\text{Ta})$ to those of the other γ resonances (X), measured for the same pair of host metals.

		4d-5d host-metal pairs					
		Nb-Ta	Mo-W	Ru-Os	Rh-Ir	Pd-Pt	Refs.
(a)							
	^{181}Ta	-15.18 ± 0.11	-21.64 ± 0.11	-25.15 ± 0.35	-26.96 ± 0.30	-30.46 ± 0.30	this work
	^{197}Au	0.28 ± 0.03	0.75 ± 0.05	0.91 ± 0.05	1.00 ± 0.07	1.04 ± 0.04	12, 26-28
ΔS	^{193}Ir	0.27 ± 0.04	0.37 ± 0.08	0.43 ± 0.02	0.62 ± 0.02	0.65 ± 0.03	28
(mm/sec)	^{99}Ru	0.055 ± 0.011	0.092 ± 0.010	0.109 ± 0.005	0.121 ± 0.009	0.123 ± 0.014	12, 26-28
	^{57}Fe	-0.06 ± 0.02	-0.09 ± 0.01	-0.06 ± 0.02	-0.11 ± 0.01	-1.17 ± 0.01	25, 30-32
(b)							
	$X = ^{197}\text{Au}$	-54 ± 6	-29 ± 2	-28 ± 2	-27 ± 2	-29 ± 2	
$\Delta S(^{181}\text{Ta})$	$X = ^{193}\text{Ir}$	-57 ± 10	-59 ± 14	-58 ± 3	-44 ± 2	-47 ± 3	
$\Delta S(X)$	$X = ^{99}\text{Ru}$	-276 ± 57	-235 ± 27	-231 ± 14	-223 ± 19	-248 ± 31	
	$X = ^{57}\text{Fe}$	253 ± 84	240 ± 27	419 ± 140	245 ± 22	179 ± 10	

Table IV summarizes the experimental isomer-shift differences (ΔS) between homologous $4d$ and $5d$ transition-metal hosts for γ resonances of ^{197}Au , ^{193}Ir , ^{99}Ru , ^{57}Fe , and ^{181}Ta . In the lower part of the table, the ratios of ΔS for ^{181}Ta to those measured for other γ resonances (X) between the same pair of host metals, are listed. With only a few exceptions, these ratios are remarkably constant within the limits of error for a given pair of γ resonances. This means that the differences of electron densities measured with different transition-metal impurities for various homologous $4d$ - $5d$ host-metal pairs are approximately proportional to each other. If the proportionality factors can be estimated from other data or from calculations, the ratios of isomer-shift differences listed in Table IV may be used to obtain ratios of $\Delta\langle r^2 \rangle$ for the pertinent γ resonances. We can write the following relation among the $\Delta\langle r^2 \rangle$:

$$\frac{\Delta\langle r^2 \rangle_1}{\Delta\langle r^2 \rangle_2} = \frac{E_1 Z_2 \Delta S_1 \rho_2}{E_2 Z_1 \Delta S_2 \rho_1} \quad (2)$$

Here the indices 1 and 2 refer to two separate γ resonances with energies E_1 and E_2 in elements with atomic numbers Z_1 and Z_2 , respectively. ρ_2/ρ_1 stands for the ratio of the electron density difference at impurity element 2 to that at impurity element 1 for the two chemical environments in question.

The problem consists in obtaining numbers for the ratio of electron density differences between homologous $5d$ and $4d$ host metals. This ratio will be abbreviated in the following by $R_{da}(1, 2) = \rho_2/\rho_1$, where the subscript da stands for dilute alloys. We cannot directly derive values for R_{da} from the results of free-ion self-consistent-field calculations, without making certain assumptions on the relative strengths of the effective $d \rightarrow s$ electron transfer, which occurs in the charge distribution at an impurity atom when transferring it from a $5d$

transition-metal host to the homologous $4d$ host.

One way of gaining information on the relative strengths of these effective $d \rightarrow s$ electron transfers is to compare the ratios of isomer-shift differences for dilute alloys, $(\Delta S_1/\Delta S_2)_{da}$, with ratios of isomer-shift differences between isoelectronic configurations of the two elements, $(\Delta S_1/\Delta S_2)_{ie}$.³⁷ The ratios of electron density differences between isoelectronic configurations, abbreviated by R_{ie} , can be obtained from the results of free-ion self-consistent-field calculations. It is obvious that the following relation holds:

$$R_{da}(1, 2) = R_{ie}(1, 2) \left(\frac{\Delta S_1}{\Delta S_2} \right)_{da} / \left(\frac{\Delta S_1}{\Delta S_2} \right)_{ie} \quad (3)$$

Unfortunately, the concept of isoelectronic compounds³⁷ cannot yet be applied to the ^{181}Ta case, since too few compounds of tantalum have been studied. In the case of the ^{57}Fe , ^{99}Ru , and ^{193}Ir γ resonances, however, the known systematics of isomer shifts for chemical compounds³⁸ allow an application of this concept. Using Eq. (3) and the R_{ie} ratios as derived from the results of free-ion self-consistent-field calculations we can then derive the ratios R_{da} for impurity elements of Ir, Ru, and Fe. Gold has not been included in this compar-

TABLE V. Ratios of experimental isomer-shift differences $\Delta S(X)/\Delta S(^{193}\text{Ir})$ and of electron density differences at the nucleus $R(X, \text{Ir})$ for isoelectronic configurations (ie) and for dilute alloys with homologous $5d$ and $4d$ transition metals (da), for γ resonances of ^{99}Ru (90 keV) and ^{57}Fe (14.4 keV) relative to the one of ^{193}Ir (73 keV).

X	Isoelectronic configurations		Dilute alloys with homologous $5d$ and $4d$ host metals		
	$\left(\frac{\Delta S(X)}{\Delta S(^{193}\text{Ir})} \right)_{ie}$	$R_{ie}(X, \text{Ir})$	$\left(\frac{\Delta S(X)}{\Delta S(^{193}\text{Ir})} \right)_{da}$	$R_{da}(X, \text{Ir})$	$R_{da}^*(X, \text{Ir})$
^{99}Ru	0.36	0.24	0.21	0.14	0.18
^{57}Fe	-0.54	0.15	-0.22	0.06	0.07

TABLE VI. Derivation of $\Delta\langle r^2 \rangle$ of the 6.2-keV γ resonance from systematics of isomer shifts in transition-metal hosts.

γ resonance X	$\frac{\Delta S(^{181}\text{Ta})}{\Delta S(X)}$	$R_{\text{da}}(\text{Ta}, X)$	$\frac{\Delta\langle r^2 \rangle_{\text{Ta}}}{\Delta\langle r^2 \rangle_X}$	$\Delta\langle r^2 \rangle_X$ (10^{-3} fm^2)	$\Delta\langle r^2 \rangle_{\text{Ta}}$ (10^{-3} fm^2)
^{197}Au , 77 keV	-30	0.50	-5.2	9 ^a	-47
^{193}Ir , 73 keV	-49	0.69	-6.4	4.6 ^b	-29
^{99}Ru , 90 keV	-236	5.9	-1.7	25 ^c	-43
^{57}Fe , 14.4 keV	218	11.5	2.9	-25 ^d	-72
Average:					-48

^aReference 43. ^cReference 44.
^bReference 29. ^dReference 45.

ison since it is not straightforward to associate definite electronic configurations with specific gold compounds on the basis of the measured isomer shifts.³⁹

The data are summarized in Table V. The ratios of ΔS for isoelectronic configurations (column 2) were obtained by comparing the isomer-shift differences for compounds with isoelectronic configurations.^{27,38} The R_{1e} ratios, which are presented in column 3, were derived from the results of relativistic Dirac-Fock calculations for Ru⁴⁰ and of nonrelativistic Hartree-Fock calculations for Fe⁴¹ and Ir.⁴² Using our experimental values for the ratios of dilute-alloy isomer-shift differences (the values listed in column 4 are weighted mean values of the individual ratios given in Table IV) we can derive, with the help of Eq. (3), ratios of the electron density differences between homologous $5d$ and $4d$ host metals (column 5). In the last column of Table V ratios of electron density differences, called R_{da}^* , are also given, which were directly derived from the results of free-ion self-consistent-field calculations on the assumption that the magnitudes of the effective $d \rightarrow s$ electron transfer from $5d$ to homologous $4d$ host metals are the same for impurity atoms of ^{57}Fe , ^{99}Ru , and ^{193}Ir . The deviations of R_{da}^* from R_{da} are less than about 30%, indicating that the assumption of constant $d \rightarrow s$ electron transfer is approximately valid within the present accuracy for these three impurity elements.

This result indicates that we can make the assumption of constant effective $d \rightarrow s$ electron transfer for impurity atoms of Ta, Ir, and Au. We are then in a position to calculate numbers for $R_{\text{da}}(\text{Ta}, \text{Ir})$ and $R_{\text{da}}(\text{Ta}, \text{Au})$, using the results of free-ion self-consistent-field calculations for tantalum and gold.⁴⁰

Table VI summarizes the data we have employed for deriving estimates of $\Delta\langle r^2 \rangle$ for the 6.2-keV γ transition. In column 2 the weighted mean values of the individual ratios $\Delta S(^{181}\text{Ta})/\Delta S(X)$, given in Table IV, are listed for the four γ resonances under discussion relative to the one of ^{181}Ta . The

ratios of electron density differences $R_{\text{da}}(\text{Ta}, X)$, given in column 3, were obtained as described above. For $R_{\text{da}}(\text{Ta}, \text{Ir})$ and $R_{\text{da}}(\text{Ta}, \text{Au})$ the concept of approximately constant $d \rightarrow s$ charge transfer was employed, while the number for $R_{\text{da}}(\text{Ta}, \text{Ru})$ and $R_{\text{da}}(\text{Ta}, \text{Fe})$ were obtained by dividing $R_{\text{da}}(\text{Ta}, \text{Ir})$ by the results of Table V, column 5. With these numbers for $R_{\text{da}}(\text{Ta}, X)$, the ratios of $\Delta\langle r^2 \rangle$ presented in column 4 are derived, using Eq. (2). The $\Delta\langle r^2 \rangle$ values for the γ resonances of ^{197}Au , ^{193}Ir , ^{99}Ru , and ^{57}Fe , as listed in column 5, were taken from Refs. 43, 29, 44, and 45, respectively. The absolute accuracy of these numbers should not be overestimated, as is most clearly expressed by the fact that the published values for $\Delta\langle r^2 \rangle$ of the 14.4-keV γ transition of ^{57}Fe range from -9×10^{-3} to $-52 \times 10^{-3} \text{ fm}^2$.⁴⁵⁻⁵² The four estimates of $\Delta\langle r^2 \rangle$ of the 6.2-keV γ resonance are finally given in the last column of Table VI. As a final result for $\Delta\langle r^2 \rangle$ we take the mean value

$$\Delta\langle r^2 \rangle = -5 \times 10^{-2} \text{ fm}^2 .$$

The error of this value can only be estimated, especially since it is directly correlated with the uncertainties of the $\Delta\langle r^2 \rangle$ values from which it was derived. We think, however, that 50% is an upper limit to this error.

This is one of the largest changes in nuclear-charge radius observed until now for Mössbauer transition.²⁹ It is associated with a single-particle proton transition between the 6.2-keV level and the ground state, which are both intrinsic proton states of the strongly deformed ^{181}Ta nucleus, with Nilsson assignments $\frac{7}{2}^+$ [404] and $\frac{9}{2}^-$ [514], respectively.

It has been pointed out earlier^{5,12,13} that part of this large negative value for $\Delta\langle r^2 \rangle$ may be due to a small decrease in deformation upon nuclear excitation. Using the experimental result for the ratio of nuclear quadrupole moments, $Q(\frac{9}{2}^-)/Q(\frac{7}{2}^+) = 1.133 \pm 0.010$,⁸ and the assumption of constant nuclear volume in both states, a value of $\Delta\langle r^2 \rangle = -(4.4 \pm 1.3) \times 10^{-2} \text{ fm}^2$ is obtained for this collective contribution. The close agreement between this number and our experimental result should, however, not be taken too seriously, since this model is very crude, and in addition completely neglects single-particle contributions to $\Delta\langle r^2 \rangle$. It is hoped that in the near future microscopic calculations of $\Delta\langle r^2 \rangle$ will become available for this Mössbauer transition.

C. Isomer Shifts in Tantalum Compounds

With the sign and magnitude of $\Delta\langle r^2 \rangle$ established we can now discuss the isomer shifts measured for the pentavalent ABO_3 compounds LiTaO_3 , NaTaO_3 , and KTaO_3 and for TaC.

1. Alkali Tantalates of the Form ABO_3

With a negative sign for $\Delta\langle r^2 \rangle$, the isomer-shift results show that ρ decreases from LiTaO_3 to NaTaO_3 to KTaO_3 . Such a trend in ρ can be expected from the chemical bonding in these alkali tantalates, taking into account their ferroelectric properties.⁵³

The lattice structures of these tantalates are known: LiTaO_3 is hexagonal, NaTaO_3 is orthorhombic, and KTaO_3 has the cubic perovskite structure.^{54,55} The $B-O$ bond lengths increase from LiTaO_3 to NaTaO_3 to KTaO_3 . LiTaO_3 is a displacement ferroelectric with a Curie point at 665°C ,⁵³ while NaTaO_3 has probably an antiferroelectric phase transition at 480°C .⁵⁶ For KTaO_3 , no ferroelectric behavior has been found down to 1.6 K .⁵⁷

The bonding in ABO_3 ferroelectric crystals with a perovskite-type structure may be described by partly ionic $B-O$ bonds with appreciable covalent contributions.⁵⁸ In the present context only the $B-O$ bonds have to be considered, since the B ions are highly screened from the A ions by the oxygen octahedra. It has been shown that for compounds with the same ferroactive cation an increase in the degree of covalency of its bonds with oxygen will lead to an increase in the ferroelectric transition temperature.⁵⁹ Applied to the present case, this means that the degree of covalency of the $B-O$ bonds should decrease from LiTaO_3 to NaTaO_3 to KTaO_3 . Such a trend is also expected from the bond lengths which are increasing in this direction.

Within a given oxidation state the electron density at the Ta nucleus is expected to increase with increasing covalency owing to the expectedly positive direct contribution of σ -bonding orbitals to ρ . Such a dependence of ρ on covalency has previously been observed for Au(I) and Au(III) compounds,³⁹ as well as for compounds of Ir, Os, and Ru.^{38,60,61} The electron density is therefore expected to decrease from LiTaO_3 to NaTaO_3 to KTaO_3 with decreasing covalent character of the $B-O$ bonds. This is in agreement with observation if one takes the negative sign for $\Delta\langle r^2 \rangle$.

2. Tantalum Monocarbide

Common to all nitrides and carbides of group-IV and -V transition metals are high melting points, extreme hardness and brittleness, and good metallic conductivity. Because of this unusual combination of physical properties, the electronic structures of these so-called hard refractory metals are of considerable interest.²⁴

TaC exists over a wide range of compositions, with most of its physical properties varying smoothly with the molar ratio. The two TaC samples studied in the present work had a chemical compo-

sition close to stoichiometry. With a negative sign for $\Delta\langle r^2 \rangle$, the present isomer-shift results (Fig. 6) show that ρ is smaller for TaC than for any other of the studied environments of tantalum.

Considering the rather similar physical properties of TaC and of the homologous $4d$ -compound NbC, a decrease in ρ relative to the metal and the pentavalent compounds may be expected from the results of recent self-consistent augmented-plane-wave band-structure calculations for NbC.⁶² These calculations show that the occupied states of the conduction band of NbC have predominantly d character with only small p and even less s character. A similar band structure should be expected for TaC. On the other hand, the conduction electrons of tantalum metal possess more s character.⁶³ Using d -electron shielding arguments, a smaller ρ is therefore expected for TaC than for the metal. This is qualitatively in agreement with our experimental results, if we take a negative sign for $\Delta\langle r^2 \rangle$. For a more quantitative analysis of the measured isomer shift, band-structure calculations for TaC would be needed.

V. CONCLUSIONS

With the experimental results of the present work, resolution in Mössbauer isomer-shift studies has increased by more than an order of magnitude. This is basically caused by a coincidence of three highly favorable properties of this γ resonance, namely, the small natural linewidth of the 6.2-keV γ rays, the large magnitude of $\Delta\langle r^2 \rangle$, and the high atomic number of tantalum.

This improved resolution should be of great interest for solid-state applications of Mössbauer isomer-shift studies, since small changes in the total electron density at the nucleus can be measured with an otherwise unreached precision. This increased sensitivity could be especially useful in Mössbauer studies of phase transitions.

Some other peculiarities of the ^{181}Ta γ resonance are partly connected with the low transition energy, which is the lowest one of all presently studied Mössbauer γ rays. As a consequence, Mössbauer absorption should be observable over an unusually large temperature region. In such applications the low γ -ray energy and the large nuclear mass of ^{181}Ta result in relatively small thermal red shifts. Owing to the high sensitivity to changes in ρ , solid-state effects will therefore completely dominate the experimentally observed variation of the transition energy with temperature. This has recently been demonstrated in a study of temperature shifts for dilute impurities of ^{181}Ta in transition-metal hosts.²¹

One should keep in mind that the present resolution was reached with experimental linewidths typically of the order of 10–100 times twice the natur-

al one. Even though many applications may be achieved with the present linewidths, an improvement in this respect would, of course, be of great interest.

ACKNOWLEDGMENTS

The authors would like to thank D. A. Shirley, G. M. Kalvius, and R. L. Mössbauer for valuable

discussions as well as for continuous support of this work. They are also indebted to J. B. Mann and K. Schwarz for communication of theoretical results prior to publication. One of the authors (G. K.) would like to thank the Miller Institute for Basic Research in Science at the University of California, Berkeley, for a postdoctoral research fellowship.

- *Supported in part by the U.S. Atomic Energy Commission and the Deutsche Forschungsgemeinschaft.
- [†]Present address: Physik-Department E15, Technische Universität München, D-8046 Garching, Germany.
- ¹H. de Waard and G. J. Perlow, *Phys. Rev. Lett.* **24**, 566 (1970).
- ²W. A. Steyert, R. D. Taylor, and E. K. Storms, *Phys. Rev. Lett.* **14**, 739 (1965).
- ³C. Sauer, E. Matthias, and R. L. Mössbauer, *Phys. Rev. Lett.* **21**, 961 (1968).
- ⁴C. Sauer, *Z. Phys.* **222**, 439 (1969); and references therein.
- ⁵G. Kaindl and D. Salomon, *Perspectives in Mössbauer Effect Spectroscopy*, edited by S. G. Cohen and M. Pasternak (Plenum, New York, to be published).
- ⁶G. Kaindl and D. Salomon, University of California, Lawrence Berkeley Laboratory Report No. UCRL-20426, 1970, p. 215 (unpublished).
- ⁷G. Kaindl and D. Salomon, *Phys. Lett. A* **42**, 333 (1973).
- ⁸G. Kaindl, D. Salomon, and G. Wortmann, *Phys. Rev. Lett.* **28**, 952 (1972).
- ⁹G. Kaindl and D. Salomon, *Phys. Lett. A* **40**, 179 (1972).
- ¹⁰G. Kaindl and D. Salomon, *Bull. Am. Phys. Soc.* **17**, 681 (1972).
- ¹¹G. Wortmann, *Phys. Lett. A* **35**, 391 (1971).
- ¹²D. Salomon, Ph.D. thesis, Lawrence Berkeley Laboratory Report No. LBL-1276 (1972) (unpublished).
- ¹³G. Wortmann, Ph.D. thesis (Technische Universität München, 1971) (unpublished).
- ¹⁴D. Salomon, G. Kaindl, and D. A. Shirley, *Phys. Lett. A* **36**, 457 (1971).
- ¹⁵G. Kaindl and D. Salomon, *Phys. Lett. B* **32**, 364 (1970).
- ¹⁶E. H. Hopkins, D. T. Peterson, and N. Baker, Iowa State University Report No. IS-1184, 1966 (unpublished).
- ¹⁷The authors are indebted to N. H. Krikorian (Los Alamos Scientific Laboratory, University of California) and to J. J. Nickel and V. Gotthardt (Institut für Festkörperchemie, Universität München) for supplying high-purity TaC samples.
- ¹⁸G. Kaindl, M. R. Maier, H. Schaller, and F. Wagner, *Nucl. Instrum. Methods* **66**, 277 (1968).
- ¹⁹G. T. Trammel and J. T. Hannon, *Phys. Rev.* **180**, 337 (1969).
- ²⁰Yu. M. Kagan, A. M. Afanas'ev, and V. K. Vojtovetskii, *Zh. Eksp. Teor. Fiz. Pis'ma Red.* **9**, 155 (1969) [*JETP Lett.* **9**, 91 (1969)].
- ²¹G. Kaindl and D. Salomon, *Phys. Rev. Lett.* **30**, 579 (1973).
- ²²R. D. Taylor and E. K. Storms, *Bull. Am. Phys. Soc.* **14**, 836 (1969).
- ²³*Gmelins Handbuch der Anorganischen Chemie*, edited by Gmelin-Institut (Verlag Chemie, Weinheim/Bergstrasse, 1969), Vol. 50.
- ²⁴L. E. Toth, *Transition Metal Carbides and Nitrides* (Academic, New York, 1971).
- ²⁵S. M. Quaim, *Proc. Phys. Soc. Lond.* **90**, 1065 (1967).
- ²⁶G. Kaindl and D. Salomon, in Proceedings of the International Conference of Applications of the Mössbauer Effect, Israel, 1972 (unpublished).
- ²⁷G. Wortmann, F. E. Wagner, and G. M. Kalvius, in Ref. 26.
- ²⁸F. E. Wagner, G. Wortmann, and G. M. Kalvius, *Phys. Lett. A* **42**, 483 (1973).
- ²⁹G. K. Shenoy and G. M. Kalvius, *Hyperfine Interactions in Excited Nuclei*, edited by G. Goldring and R. Kalish (Gordon and Breach, New York, 1971), p. 1201.
- ³⁰G. Wortmann (unpublished).
- ³¹B. Window, G. Longworth, and C. E. Johnson, *J. Phys. C* **3**, 2156 (1970).
- ³²A. H. Muir, Jr., K. J. Ando, and H. M. Coogan, *Mössbauer Effect Data Index 1958-1965* (Interscience, New York, 1966).
- ³³X. A. da Silva, A. A. Gomes, and J. Danon, *Phys. Rev. B* **4**, 1161 (1971).
- ³⁴C. G. Gelatt and H. Ehrenreich, *Bull. Am. Phys. Soc.* **18**, 93 (1973).
- ³⁵O. Krogh Andersen, *Phys. Rev. B* **2**, 883 (1970).
- ³⁶Landolt-Börnstein, *New Series, Group III*, edited by K. H. Hellwege and A. M. Hellwege (Springer-Verlag, Berlin, 1971), Vol. 6.
- ³⁷S. L. Ruby, and G. K. Shenoy, *Phys. Rev.* **186**, 326 (1969).
- ³⁸G. Kaindl, D. Kucheida, W. Potzel, F. E. Wagner, U. Zahn, and R. L. Mössbauer, in Ref. 29, p. 595.
- ³⁹H. D. Bartunik, W. Potzel, R. L. Mössbauer, and G. Kaindl, *Z. Phys.* **240**, 1 (1970).
- ⁴⁰J. B. Mann (private communication).
- ⁴¹J. Blomquist, B. Ross, and M. Sundbom, *J. Chem. Phys.* **55**, 141 (1971).
- ⁴²L. W. Panek and G. J. Perlow, Argonne National Laboratory Report No. ANL-7631, 1969 (unpublished).
- ⁴³L. D. Roberts, D. O. Patterson, J. O. Thomson, and R. P. Levey, *Phys. Rev.* **179**, 656 (1969).
- ⁴⁴W. Potzel, F. E. Wagner, R. L. Mössbauer, G. Kaindl, and H. E. Seltzer, *Z. Phys.* **241**, 179 (1971).
- ⁴⁵H. Micklitz and P. H. Barret, *Phys. Rev. Lett.* **28**, 1547 (1972).
- ⁴⁶J. Danon, *Tech. Rep. Ser. IAEA* **50**, 89 (1966).
- ⁴⁷V. I. Goldanskii, in Proceedings Dubna Conference on the Mössbauer Effect, 1963 (unpublished).
- ⁴⁸E. Simánek and Z. Šroubek, *Phys. Rev.* **163**, 275 (1967).
- ⁴⁹F. Pleiter and B. Kolb, *Phys. Lett. B* **34**, 296 (1971).
- ⁵⁰T. K. McNab, H. Micklitz, and P. H. Barrett, *Phys. Rev. B* **4**, 3787 (1971).
- ⁵¹R. Rügsegger and W. Kündig, *Phys. Lett. B* **39**, 620 (1972).
- ⁵²L. R. Walker, G. K. Wertheim, and V. Jaccarino, *Phys. Rev. Lett.* **6**, 98 (1961).
- ⁵³Landolt-Börnstein, *New Series, Group III*, edited by K. H. Hellwege (Springer-Verlag, Berlin, 1969), Vol. 3.
- ⁵⁴P. Vousden, *Acta Crystallogr.* **4**, 373 (1951).
- ⁵⁵S. C. Abrahams, W. C. Hamilton, and A. Sequeira, *J. Phys. Chem. Solids* **28**, 1693 (1967).
- ⁵⁶I. G. Ismailzade, *Kristallografiya* **7**, 718 (1962) [*Sov. Phys.-Crystallogr.* **7**, 584 (1963)].
- ⁵⁷S. H. Wemple, *Phys. Rev.* **137**, A1575 (1965).
- ⁵⁸A. D. Megaw, *Acta Crystallogr.* **5**, 739 (1952); *Acta Crystallogr.* **7**, 187 (1954).
- ⁵⁹V. G. Granovskii, *Kristallografiya* **7**, 604 (1962) [*Sov. Phys.-Crystallogr.* **7**, 484 (1963)].

⁶⁰G. Kaindl, W. Potzel, F. Wagner, U. Zahn, and R. L. Mössbauer, *Z. Phys.* **226**, 103 (1969).

⁶¹F. E. Wagner and U. Zahn, *Z. Phys.* **223**, 1 (1970).

⁶²J. B. Conklin, Jr., K. Schwarz, and R. W. Simpson (private communication).

⁶³L. F. Mattheiss, *Phys. Rev. B* **1**, 373 (1970).